

## **TIME DOMAIN EFIE AND MFIE FORMULATIONS FOR ANALYSIS OF TRANSIENT ELECTROMAGNETIC SCATTERING FROM 3-D DIELECTRIC OBJECTS**

**B. H. Jung**

Department of Information and Communication Engineering  
Hoseo University  
Asan, Chungnam 336-795, Korea

**T. K. Sarkar**

Department of Electrical Engineering and Computer Science  
Syracuse University  
Syracuse, NY 13244-1240, USA

**M. Salazar-Palma**

Departamento de Senales Sistemas y Radiocomunicaciones  
Universidad Politecnica de Madrid  
Madrid 28040, Spain

**Abstract**—In this paper, we investigate various methods for solving a time-domain electric field integral equation (TD-EFIE) and a time-domain magnetic field integral equation (TD-MFIE) for analyzing the transient electromagnetic response from three-dimensional (3-D) dielectric bodies. The solution method in this paper is based on the method of moments (MoM) that involves separate spatial and temporal testing procedures. Triangular patch basis functions are used for spatial expansion and testing functions for arbitrarily shaped 3-D dielectric structures. The time-domain unknown coefficients of the equivalent electric and magnetic currents are approximated using a set of orthogonal basis functions that is derived from the Laguerre functions. These basis functions are also used as the temporal testing. Numerical results involving equivalent currents and far fields computed by the proposed TD-EFIE and TD-MFIE formulations are presented and compared.

## 1 Introduction

## 2 Integral Equations

### 3 Solution Methods for TD-EFIE

3.1 TD-EFIE (1):  $\mathbf{e}$  and  $\mathbf{h}$  Formulation

3.2 TD-EFIE (2):  $\mathbf{e}$  and  $\mathbf{M}$  Formulation

3.3 TD-EFIE (3):  $\mathbf{J}$  and  $\mathbf{M}$  Formulation

### 4 Solution Methods for TD-MFIE

4.1 TD-MFIE (1):  $\mathbf{h}$  and  $\mathbf{e}$  Formulation

4.2 TD-MFIE (2):  $\mathbf{h}$  and  $\mathbf{J}$  Formulation

4.3 TD-MFIE (3):  $\mathbf{M}$  and  $\mathbf{J}$  Formulation

## 5 Numerical Example

## 6 Conclusion

## Acknowledgment

## References

## 1. INTRODUCTION

For the solution of a time-domain integral equation, the marching-on in time (MOT) method is usually employed [1]. A serious drawback of this algorithm is the occurrence of late-time instabilities in the form of high frequency oscillation. Several MOT formulations have been presented for the solution of the electromagnetic scattering from arbitrarily shaped 3-D structures using triangular patch modeling technique [2–9]. An explicit solution has been presented by differentiating the coupled integral equations and using second order finite difference [2–9]. But the results become unstable for late times. Its late-time oscillations could be eliminated by approximating the average value of the current. In addition, a backward finite difference approximation for the magnetic vector potential term has been used for the implicit technique to minimize these late-time oscillations [7, 10]. Even though employing the implicit technique, the solution obtained by using MOT has still late-time oscillation that is dependent on the choice of the time step. For perfectly conducting bodies, a central finite difference methodology with the TD-EFIE is presented to improve the stability and the accuracy of the solution [8]. Even after all these modifications used in [8], when one applies it to analyze dielectric structures, one is not guaranteed to obtain a stable solution.

In this paper, we survey various methods for solving TD-EFIE and TD-MFIE to obtain stable responses from arbitrarily shaped 3-D dielectric objects using Laguerre polynomials as temporal basis functions, based on the recent work [11]. The Laguerre series is defined only over the interval from zero to infinity, and hence, is considered to be more suited for handling transient problems, as it naturally enforces causality. Using the Laguerre polynomials, we construct a set of orthonormal basis functions [12]. Transient quantities that are functions of time can be spanned in terms of these orthogonal basis functions. The temporal basis functions used in this work decay to zero as time increases to infinity. Therefore, transient response spanned by these basis functions is also merge to zero as time progresses. Using Galerkin's method, we introduce a temporal testing procedure, which is similar to the spatial testing procedure of the MoM. By applying the temporal testing to the TD-EFIE and TD-MFIE, one can eliminate the numerical instabilities. Instead of the MOT procedure, we employ a marching-on in-degree procedure by increasing the degree of the temporal testing functions. Therefore, one can obtain the unknown coefficients of the expansion by solving a matrix equation recursively with a finite number of basis functions. In the next section, we describe the TD-EFIE and TD-MFIE. In Sections 3 and 4, we set up the matrix equations by applying MoM with spatial and temporal testing procedures. Section 5 presents and compares numerical results followed by Section 6, the conclusion.

## 2. INTEGRAL EQUATIONS

In this section, we discuss the TD-EFIE and TD-MFIE using the induced equivalent currents on the dielectric scatterer. Consider a homogeneous dielectric body with a permittivity  $\epsilon_2$  and a permeability  $\mu_2$  placed in an infinite homogeneous medium with a permittivity

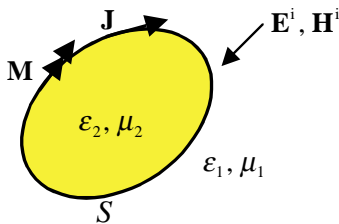


**Figure 1.** Homogeneous dielectric body illuminated by an electromagnetic pulse.

$\varepsilon_1$  and a permeability  $\mu_1$  as shown in Fig. 1. By invoking the equivalence principle, the integral equations are formulated in terms of the equivalent electric and magnetic current  $\mathbf{J}$  and  $\mathbf{M}$  on the surface  $S$  of the dielectric body. By enforcing the continuity of the tangential electric and magnetic field at  $S$ , the following TD-EFIE and TD-MFIE are obtained:

$$\begin{aligned} & \left[ \frac{\partial}{\partial t} \mathbf{A}_v(\mathbf{r}, t) + \nabla \Phi_v(\mathbf{r}, t) + \frac{1}{\varepsilon_v} \nabla \times \mathbf{F}_v(\mathbf{r}, t) \right]_{\text{tan}} \\ &= \begin{cases} [\mathbf{E}^i(\mathbf{r}, t)]_{\text{tan}}, & v = 1 \\ 0, & v = 2 \end{cases}, \quad \mathbf{r} \in S \end{aligned} \quad (1)$$

$$\begin{aligned} & \left[ \frac{\partial}{\partial t} \mathbf{F}_v(\mathbf{r}, t) + \nabla \Psi_v(\mathbf{r}, t) - \frac{1}{\mu_v} \nabla \times \mathbf{A}_v(\mathbf{r}, t) \right]_{\text{tan}} \\ &= \begin{cases} [\mathbf{H}^i(\mathbf{r}, t)]_{\text{tan}}, & v = 1 \\ 0, & v = 2 \end{cases}, \quad \mathbf{r} \in S \end{aligned} \quad (2)$$

where  $\mathbf{E}^i$  and  $\mathbf{H}^i$  are the incident electric and magnetic fields, respectively. The subscript 'tan' denotes the tangential component. In (1) and (2),  $\mathbf{A}_v$  and  $\mathbf{F}_v$  are the magnetic and electric vector potentials, respectively, and  $\Phi_v$  and  $\Psi_v$  are the electric and magnetic scalar potentials given by

$$\mathbf{A}_v(\mathbf{r}, t) = \frac{\mu_v}{4\pi} \int_S \frac{\mathbf{J}(\mathbf{r}', \tau_v)}{R} dS' \quad (3)$$

$$\mathbf{F}_v(\mathbf{r}, t) = \frac{\varepsilon_v}{4\pi} \int_S \frac{\mathbf{M}(\mathbf{r}', \tau_v)}{R} dS' \quad (4)$$

$$\Phi_v(\mathbf{r}, t) = \frac{1}{4\pi\varepsilon_v} \int_S \frac{q_e(\mathbf{r}', \tau_v)}{R} dS' \quad (5)$$

$$\Psi_v(\mathbf{r}, t) = \frac{1}{4\pi\mu_v} \int_S \frac{q_m(\mathbf{r}', \tau_v)}{R} dS' \quad (6)$$

where  $R = |\mathbf{r} - \mathbf{r}'|$  represents the distance between the arbitrarily located observation point  $\mathbf{r}$  and the source point  $\mathbf{r}'$ ,  $\tau_v = t - R/c_v$  is the retarded time, and  $c_v = 1/\sqrt{\varepsilon_v\mu_v}$  is the velocity of propagation of the electromagnetic wave in the space with medium parameters  $(\varepsilon_v, \mu_v)$ . The electric and magnetic surface charge density  $q_e$  and  $q_m$  are related to the electric and magnetic current density by the equation of continuity, respectively,

$$\nabla \cdot \mathbf{J}(\mathbf{r}, t) = -\frac{\partial}{\partial t} q_e(\mathbf{r}, t) \quad (7)$$

$$\nabla \cdot \mathbf{M}(\mathbf{r}, t) = -\frac{\partial}{\partial t} q_m(\mathbf{r}, t). \quad (8)$$

The surface of the dielectric structure to be analyzed is approximated by planar triangular patches. As in [13], we define the spatial basis function associated with the  $n$ -th common edge as

$$\mathbf{f}_n(\mathbf{r}) = \mathbf{f}_n^+(\mathbf{r}) + \mathbf{f}_n^-(\mathbf{r}) \quad (9a)$$

$$\mathbf{f}_n^\pm(\mathbf{r}) = \begin{cases} \frac{l_n}{2A_n^\pm} \boldsymbol{\rho}_n^\pm, & \mathbf{r} \in T_n^\pm \\ 0, & \mathbf{r} \notin T_n^\pm \end{cases} \quad (9b)$$

where  $l_n$  and  $A_n^\pm$  are the length of the edge and the area of triangle  $T_n^\pm$ .  $\boldsymbol{\rho}_n^\pm$  is the position vector defined with respect to the free vertex of  $T_n^\pm$ . Another vector basis function associated with the  $n$ -th common edge is defined through

$$\mathbf{g}_n(\mathbf{r}) = \mathbf{g}_n^+(\mathbf{r}) + \mathbf{g}_n^-(\mathbf{r}) \quad (10a)$$

$$\mathbf{g}_n^\pm(\mathbf{r}) = \mathbf{n} \times \mathbf{f}_n^\pm(\mathbf{r}) \quad (10b)$$

where  $\mathbf{n}$  is the unit normal pointing outward from the surface at  $\mathbf{r}$ . The functions  $\mathbf{f}_n$  and  $\mathbf{g}_n$  are point-wise orthogonal in the triangle pair.

### 3. SOLUTION METHODS FOR TD-EFIE

#### 3.1. TD-EFIE (1): $e$ and $h$ Formulation

The electric current  $\mathbf{J}$  and the magnetic current  $\mathbf{M}$  on the dielectric structure may be approximated in terms of two separate spatial basis functions as

$$\mathbf{J}(\mathbf{r}, t) = \sum_{n=1}^N J_n(t) \mathbf{f}_n(\mathbf{r}) \quad (11)$$

$$\mathbf{M}(\mathbf{r}, t) = \sum_{n=1}^N M_n(t) \mathbf{g}_n(\mathbf{r}) \quad (12)$$

where  $J_n$  and  $M_n$  are constants yet to be determined and  $N$  is the number of edges on the surface for the triangulated model approximating the surface of the dielectric body. These expansions are used in the frequency-domain formulation [14, 15], and time-domain formulation [10].

When (11) is used in (1) with (5), we encounter a time-integral term which is due to (7). For convenience and to handle the time derivative of the vector potential in (1) analytically, we use a source vector  $\mathbf{e}$  introduced in [11] and [16] as

$$\mathbf{J}(\mathbf{r}, t) = \frac{\partial}{\partial t} \mathbf{e}(\mathbf{r}, t) \quad (13)$$

where the relation between this source vector and the charge density is given through

$$q_e(\mathbf{r}, t) = -\nabla \cdot \mathbf{e}(\mathbf{r}, t). \quad (14)$$

Similarly, we define another source vector for the magnetic current as

$$\mathbf{M}(\mathbf{r}, t) = \frac{\partial}{\partial t} \mathbf{h}(\mathbf{r}, t) \quad (15)$$

where the relation between this source vector and the charge densities is given through

$$q_m(\mathbf{r}, t) = -\nabla \cdot \mathbf{h}(\mathbf{r}, t). \quad (16)$$

By using (9) and (10), we may expand the two source vectors as

$$\mathbf{e}(\mathbf{r}, t) = \sum_{n=1}^N e_n(t) \mathbf{f}_n(\mathbf{r}) \quad (17)$$

$$\mathbf{h}(\mathbf{r}, t) = \sum_{n=1}^N h_n(t) \mathbf{g}_n(\mathbf{r}) \quad (18)$$

where  $e_n$  and  $h_n$  are the time domain unknown coefficients to be determined. The transient electric and magnetic current coefficients in (11) and (12) are expressed using the relation (13) and (15) with (17) and (18) as

$$J_n(t) = \frac{d}{dt} e_n(t) \quad (19)$$

$$M_n(t) = \frac{d}{dt} h_n(t). \quad (20)$$

The next step in the numerical implementation scheme is to develop a testing procedure to transform the operator equation (1) into a matrix equation using the MoM. By substituting (3)–(5) with (17) and (18), and using the standard definition of the inner product with the testing function  $\mathbf{f}_m$ , we have

$$\begin{aligned} & \sum_{n=1}^N \sum_{p,q} \left[ \mu_v a_{mn}^{pq} \frac{d^2}{dt^2} e_n(\tau_{mn,v}^{pq}) + \frac{b_{mn}^{pq}}{\varepsilon_v} e_n(\tau_{mn,v}^{pq}) \right] \\ & + \sum_{n=1}^N \left[ c_{mn}^{(v)} \frac{d}{dt} h_n(t) + \sum_{p,q} \left\{ \frac{d_{mn,1}^{pq}}{c_v} \frac{d^2}{dt^2} h_n(\tau_{mn,v}^{pq}) + d_{mn,2}^{pq} \frac{d}{dt} h_n(\tau_{mn,v}^{pq}) \right\} \right] \\ & = V_m^{E(v)}(t) \end{aligned} \quad (21)$$

where  $m = 1, 2, \dots, N$  and the elements are given by

$$a_{mn}^{pq} = \frac{1}{4\pi} \int_S \mathbf{f}_m^p(\mathbf{r}) \cdot \int_S \frac{\mathbf{f}_n^q(\mathbf{r}')}{R} dS' dS \quad (22)$$

$$b_{mn}^{pq} = \frac{1}{4\pi} \int_S \nabla \cdot \mathbf{f}_m^p(\mathbf{r}) \int_S \frac{\nabla' \cdot \mathbf{f}_n^q(\mathbf{r}')}{R} dS' dS \quad (23)$$

$$c_{mn}^{(v)} = \begin{cases} +c_{mn}, & v = 1 \\ -c_{mn}, & v = 2 \end{cases} \quad (24a)$$

$$c_{mn} = \frac{1}{2} \int_S \mathbf{f}_m(\mathbf{r}) \cdot \mathbf{n} \times \mathbf{g}_n(\mathbf{r}) dS \quad (24b)$$

$$d_{mn,k}^{pq} = \frac{1}{4\pi} \int_S \mathbf{f}_m^p(\mathbf{r}) \cdot \int_S \mathbf{g}_n^q(\mathbf{r}') \times \frac{\hat{\mathbf{R}}}{R^k} dS' dS, \quad k = 1, 2 \quad (25)$$

$$V_m^{E(v)}(t) = \begin{cases} V_m^E(t), & v = 1 \\ 0, & v = 2 \end{cases} \quad (26)$$

$$V_m^E(t) = \int_S \mathbf{f}_m(\mathbf{r}) \cdot \mathbf{E}^i(\mathbf{r}, t) dS \quad (27)$$

In deriving (21), we assume that the functions dependent on the following variable do not change appreciably within a given triangular patch so that

$$\tau_v = t - \frac{R}{c_v} \rightarrow \tau_{mn,v}^{pq} = t - \frac{R_{mn}^{pq}}{c_v}, \quad R_{mn}^{pq} = |\mathbf{r}_m^{cp} - \mathbf{r}_n^{cq}| \quad (28)$$

where  $p$  and  $q$  can be either  $+$  or  $-$ .  $\mathbf{r}_n^{c\pm}$  is the position vector of the center of triangle  $T_n^\pm$ . The integrals (22)–(27) may be evaluated by the method described in [17–23].

Now, we consider the choice of the temporal basis functions and the temporal testing procedure. An orthogonal basis function set can be derived from the Laguerre functions through the representation [12]

$$\phi_j(t) = e^{-t/2} L_j(t), \quad j = 0, 1, 2, \dots \quad (29)$$

where  $L_j$  is the Laguerre polynomial of degree  $j$  [24]. The time domain coefficients  $e_n(t)$  and  $h_n(t)$  introduced in (17) and (18), which are assumed to be causal electromagnetic response functions for  $t \geq 0$ , can be expanded using (29) as

$$e_n(t) = \sum_{j=0}^{\infty} e_{n,j} \phi_j(st) \quad (30)$$

$$h_n(t) = \sum_{j=0}^{\infty} h_{n,j} \phi_j(st) \quad (31)$$

where  $e_{n,j}$  and  $h_{n,j}$  are the coefficients to be determined, and  $s$  is a scaling factor. Using the properties of the temporal basis function (29), the expressions for the first and the second derivatives can be written explicitly using the time domain coefficient. They are available in [16] and are given by

$$\frac{d}{dt}a_n(t) = s \sum_{j=0}^{\infty} \left[ \frac{1}{2}a_{n,j} + \sum_{k=0}^{j-1} a_{n,k} \right] \phi_j(st) \quad (32)$$

$$\frac{d^2}{dt^2}a_n(t) = s^2 \sum_{j=0}^{\infty} \left[ \frac{1}{4}a_{n,j} + \sum_{k=0}^{j-1} (j-k)a_{n,k} \right] \phi_j(st) \quad (33)$$

where  $a_n(t)$  represents  $e_n(t)$  or  $h_n(t)$ , and  $a_{n,j}$  is used as  $e_{n,j}$  or  $h_{n,j}$ . Substituting the expressions for the basis functions representing the unknowns, (30) and (31), and their derivatives into (21), and performing a temporal testing, which means multiplying by  $\phi_i(st)$  and integrating from zero to infinity, we get a matrix equation as

$$\begin{bmatrix} \begin{bmatrix} \alpha_{mn}^{E(1)} \\ \alpha_{mn}^{E(2)} \end{bmatrix} & \begin{bmatrix} \beta_{mn}^{E(1)} \\ \beta_{mn}^{E(2)} \end{bmatrix} \end{bmatrix} \begin{bmatrix} [e_{n,i}] \\ [h_{n,i}] \end{bmatrix} = \begin{bmatrix} \gamma_{m,i}^{E(1)} \\ \gamma_{m,i}^{E(2)} \end{bmatrix} \quad (34)$$

where

$$\alpha_{mn}^{E(v)} = \sum_{p,q} \left( \frac{s^2 \mu_v \alpha_{mn}^{pq}}{4} + \frac{b_{mn}^{pq}}{\varepsilon_v} \right) \exp \left( -\frac{sR_{mn}^{pq}}{2c_v} \right) \quad (35)$$

$$\beta_{mn}^{E(v)} = \frac{sC_{mn}}{2} + \sum_{p,q} \left( \frac{s^2 d_{mn,1}^{pq}}{4c_v} + \frac{s d_{mn,2}^{pq}}{2} \right) \exp \left( -\frac{sR_{mn}^{pq}}{2c_v} \right) \quad (36)$$

$$\gamma_{m,i}^{E(v)} = V_{m,i}^{E(v)} + P_{m,i}^{E(v)} + Q_{m,i}^{E(v)} \quad (37)$$

$$V_{m,i}^{E(v)} = \int_0^{\infty} \phi_i(st) V_m^{E(v)}(t) d(st). \quad (38)$$

$$\begin{aligned} P_{m,i}^{E(v)} = & - \sum_{n=1}^N \sum_{p,q} \left[ \left( \frac{s^2 \mu_v \alpha_{mn}^{pq}}{4} + \frac{b_{mn}^{pq}}{\varepsilon_v} \right) \sum_{j=0}^{i-1} e_{n,j} I_{ij} \left( \frac{sR_{mn}^{pq}}{c_v} \right) \right. \\ & \left. + s^2 \mu_v \alpha_{mn}^{pq} \sum_{j=0}^i \sum_{k=0}^{j-1} (j-k) e_{n,k} I_{ij} \left( \frac{sR_{mn}^{pq}}{c_v} \right) \right] \end{aligned} \quad (39)$$

$$\begin{aligned}
Q_{m,i}^{E(v)} = & - \sum_{n=1}^N \left[ sC_{mn}^{(v)} \sum_{k=0}^{i-1} h_{n,k} \right. \\
& + \sum_{p,q} \left\{ \left( \frac{s^2 d_{mn,1}^{pq}}{4c_v} + \frac{s d_{mn,2}^{pq}}{2} \right) \sum_{j=0}^{i-1} h_{n,j} I_{ij} \left( \frac{sR_{mn}^{pq}}{c_v} \right) \right. \\
& + \frac{s^2 d_{mn,1}^{pq}}{c_v} \sum_{j=0}^i \sum_{k=0}^{j-1} (j-k) h_{n,k} I_{ij} \left( \frac{sR_{mn}^{pq}}{c_v} \right) \\
& \left. \left. + s d_{mn,2}^{pq} \sum_{j=0}^i \sum_{k=0}^{j-1} h_{n,k} I_{ij} \left( \frac{sR_{mn}^{pq}}{c_v} \right) \right\} \right]. \quad (40)
\end{aligned}$$

$$I_{ij} \left( \frac{sR_{mn}^{pq}}{c_v} \right) = \phi_{i-j} \left( \frac{sR_{mn}^{pq}}{c_v} \right) - \phi_{i-j-1} \left( \frac{sR_{mn}^{pq}}{c_v} \right), \quad j \leq i. \quad (41)$$

A similar procedure to obtain (34)–(41) can be found in detail in [16].

By solving the matrix equation (34) using a LU decomposition, in a marching-on in degree manner with  $M$  temporal basis functions, the electric and magnetic transient current coefficients (19) and (20) are expressed using (32) [11, 16]. Once the equivalent currents on the dielectric scatterer have been determined, we can compute the far scattered fields. These fields may be thought as the superposition of the fields due to the electric currents only and with the fields due to the magnetic currents only. We present an analytic method to compute the far fields directly by using the coefficient  $e_n(t)$  and  $h_n(t)$  obtained from (34). The scattered field due to the electric currents alone at a point  $\mathbf{r}$  is given by

$$\mathbf{E}_{\mathbf{J}}^s(\mathbf{r}, t) \approx -\frac{\partial}{\partial t} \mathbf{A}(\mathbf{r}, t) \quad (42)$$

where the subscript  $\mathbf{J}$  refers to the electric current. Substituting (3), (13), and (17) into (42) with (9a), we get

$$\mathbf{E}_{\mathbf{J}}^s(\mathbf{r}, t) \approx -\frac{\mu_1}{4\pi} \sum_{n=1}^N \sum_q \int_S \frac{d^2}{dt^2} e_n(\tau) \frac{\mathbf{f}_n^q(\mathbf{r}')}{R} dS'. \quad (43)$$

We make the following approximations for the far field calculations:

$$\begin{aligned}
R &\approx r - \mathbf{r}' \cdot \hat{\mathbf{r}} && \text{for the time retardation term } t - R/c_1 \\
R &\approx r && \text{for the amplitude term } 1/R
\end{aligned}$$

where  $\hat{\mathbf{r}} = \mathbf{r}/r$  is a unit vector in the direction of the radiation. The integral in (43) is evaluated by approximating the integrand by the

value at the center of the source triangle  $T_n^q$ . Substituting (9b) into (43) and approximating  $\mathbf{r}' \approx \mathbf{r}_n^{cq}$  and  $\boldsymbol{\rho}_n^q \approx \boldsymbol{\rho}_n^{cq}$ , we obtain

$$\mathbf{E}_J^s(\mathbf{r}, t) \approx -\frac{\mu_1}{8\pi r} \sum_{n=1}^N l_n \sum_q \boldsymbol{\rho}_n^{cq} \frac{d^2}{dt^2} e_n(\tau_n^q) \quad (44)$$

where  $\tau_n^q \approx t - (r - \mathbf{r}_n^{cq} \cdot \hat{\mathbf{r}})/c_1$ . The scattered magnetic field is given by

$$\mathbf{H}_M^s(\mathbf{r}, t) \approx -\frac{\partial}{\partial t} \mathbf{F}(\mathbf{r}, t) \quad (45)$$

where the subscript  $M$  refers to the magnetic current. By following a similar analysis as that for the electric currents or applying the duality theorem to (43), the far magnetic field is given by

$$\begin{aligned} \mathbf{H}_M^s(\mathbf{r}, t) &\approx -\frac{\varepsilon_1}{4\pi} \sum_{n=1}^N \sum_q \int_S \frac{d^2}{dt^2} h_n(\tau) \frac{\mathbf{g}_n^q(\mathbf{r})}{R} dS' \\ &= -\frac{\varepsilon_1}{8\pi r} \sum_{n=1}^N l_n \sum_q \mathbf{n} \times \boldsymbol{\rho}_n^{cq} \frac{d^2}{dt^2} h_n(\tau_n^q) \end{aligned} \quad (46)$$

where  $\mathbf{n}$  is the unit normal pointing outward from the triangle  $T_n^q$ . From (46), the electric field is

$$\mathbf{E}_M^s(\mathbf{r}, t) = \eta_1 \mathbf{H}_M^s(\mathbf{r}, t) \times \hat{\mathbf{r}} \quad (47)$$

where  $\eta_1$  is the wave impedance in the medium surrounding the scatterer. Finally the total field scattered from the dielectric body may be obtained by adding (44) and (47) as

$$\mathbf{E}^s(\mathbf{r}, t) \approx -\frac{1}{8\pi c_1 r} \sum_{n=1}^N l_n \sum_q \left[ \eta_1 \boldsymbol{\rho}_n^q \frac{d^2}{dt^2} e_n(\tau_n^q) + (\mathbf{n} \times \boldsymbol{\rho}_n^q) \frac{d^2}{dt^2} h_n(\tau_n^q) \times \hat{\mathbf{r}} \right]. \quad (48)$$

The second derivative of the time domain coefficient is obtained from (33) with  $M - 1$  as the upper limit of summation over  $j$  instead of  $\infty$ .

### 3.2. TD-EFIE (2): $e$ and $M$ Formulation

In this section, we consider the second method using the expansion of magnetic current (12) directly instead of using (18). The time-domain magnetic current coefficient is expanded as [11]

$$M_n(t) = \sum_{j=0}^{\infty} M_{n,j} \phi_j(st). \quad (49)$$

Substituting (12) and (49) into the third term of the left hand side in (1) and following a similar analysis as that for (34), we have a matrix equation

$$\begin{bmatrix} \left[ \begin{array}{c} \alpha_{mn}^{E(1)} \\ \alpha_{mn}^{E(2)} \end{array} \right] & \left[ \begin{array}{c} \beta_{mn}^{E(1)} \\ \beta_{mn}^{E(2)} \end{array} \right] \end{bmatrix} \begin{bmatrix} [e_{n,i}] \\ [M_{n,i}] \end{bmatrix} = \begin{bmatrix} \left[ \begin{array}{c} \gamma_{m,i}^{E(1)} \\ \gamma_{m,i}^{E(2)} \end{array} \right] \end{bmatrix} \quad (50)$$

where the elements related to the magnetic current coefficient are

$$\begin{aligned} \beta_{mn}^{E(v)} &= c_{mn}^{(v)} + \sum_{p,q} \left( \frac{sd_{mn,1}^{pq}}{2c_v} + d_{mn,2}^{pq} \right) \exp \left( -\frac{sR_{mn}^{pq}}{2c_v} \right) \\ Q_{m,i}^{E(v)} &= - \sum_{n=1}^N \sum_{p,q} \left\{ \left( \frac{sd_{mn,1}^{pq}}{2c_v} + d_{mn,2}^{pq} \right) \sum_{j=0}^{i-1} M_{n,j} I_{ij} \left( \frac{sR_{mn}^{pq}}{c_v} \right) \right. \\ &\quad \left. + \frac{sd_{mn,1}^{pq}}{c_v} \sum_{j=0}^i \sum_{k=0}^{j-1} M_{n,j} I_{ij} \left( \frac{sR_{mn}^{pq}}{c_v} \right) \right\} \end{aligned} \quad (51)$$

and other elements related to the coefficient  $e_{n,i}$  are similar to those used in (34) of the previous section. By solving (50) by a marching-on in degree algorithm with  $M$  temporal basis functions, we can obtain the magnetic current coefficient directly in (49), and the far field takes the following form:

$$\mathbf{E}^s(\mathbf{r}, t) \approx -\frac{1}{8\pi c_1 r} \sum_{n=1}^N l_n \sum_q \left[ \eta_1 \boldsymbol{\rho}_n^q \frac{d^2}{dt^2} e_n(\tau_n^q) + (\mathbf{n} \times \boldsymbol{\rho}_n^q) \frac{d}{dt} M_n(\tau_n^q) \times \hat{\mathbf{r}} \right]. \quad (53)$$

### 3.3. TD-EFIE (3): $J$ and $M$ Formulation

In this section, we present a third method using the expansion for the equivalent currents directly instead of using the two source vectors. Taking a derivative with respect to time, we derive the following integral equations from (1)

$$\begin{aligned} &\left[ \frac{\partial^2}{\partial t^2} \mathbf{A}_v(\mathbf{r}, t) + \nabla \frac{\partial}{\partial t} \Phi_v(\mathbf{r}, t) + \frac{1}{\varepsilon_v} \nabla \times \frac{\partial}{\partial t} \mathbf{F}_v(\mathbf{r}, t) \right]_{\tan} \\ &= \begin{cases} \left[ \frac{\partial}{\partial t} \mathbf{E}^i(\mathbf{r}, t) \right]_{\tan} & v = 1 \\ 0, & v = 2 \end{cases} \quad \mathbf{r} \in S. \end{aligned} \quad (54)$$

Using (11) and (12), the electric current coefficient is expanded as

$$J_n(t) = \sum_{j=0}^{\infty} J_{n,j} \phi_j(st) \quad (55)$$

where  $J_{n,j}$  is the coefficient to be determined, and the magnetic current coefficient is expanded as (49). Substituting (49) and (55) with (3)–(5) into (54), and following a similar procedure as that for (34), we have a matrix equation

$$\begin{bmatrix} \begin{bmatrix} E^{(1)} \\ \alpha_{mn} \end{bmatrix} \\ \begin{bmatrix} E^{(2)} \\ \alpha_{mn} \end{bmatrix} \end{bmatrix} \begin{bmatrix} \begin{bmatrix} \beta_{mn}^{E(1)} \end{bmatrix} \\ \begin{bmatrix} \beta_{mn}^{E(2)} \end{bmatrix} \end{bmatrix} \begin{bmatrix} \begin{bmatrix} J_{n,i} \end{bmatrix} \\ \begin{bmatrix} M_{n,i} \end{bmatrix} \end{bmatrix} = \begin{bmatrix} \begin{bmatrix} \gamma_{m,i}^{E(1)} \end{bmatrix} \\ \begin{bmatrix} \gamma_{m,i}^{E(2)} \end{bmatrix} \end{bmatrix} \quad (56)$$

where the matrix elements in the left hand side are same to those used in (34) in the Section 3.1, and the elements related to the right hand side are obtained by replacing  $J_{n,j}$  and  $M_{n,j}$  instead of  $e_{n,j}$  and  $h_{n,j}$  in (37)–(41), respectively, and

$$V_m^E(t) = \int_S \mathbf{f}_m(\mathbf{r}) \cdot \frac{\partial}{\partial t} \mathbf{E}^i(\mathbf{r}, t) dS. \quad (57)$$

By solving (56) with a marching-on in degree algorithm with  $M$  temporal basis functions, we can obtain the magnetic and electric current coefficients directly as given in (49) and (55) by replacing  $M-1$  instead of  $\infty$ . The far field is obtained as following:

$$\mathbf{E}^s(\mathbf{r}, t) \approx -\frac{1}{8\pi c_1 r} \sum_{n=1}^N l_n \sum_q \left[ \eta_1 \boldsymbol{\rho}_n^q \frac{d}{dt} J_n(\tau_n^q) + (\mathbf{n} \times \boldsymbol{\rho}_n^q) \frac{d}{dt} M_n(\tau_n^q) \times \hat{\mathbf{r}} \right]. \quad (58)$$

The first derivative of the equivalent current coefficients is given in (32) with  $M-1$  as the upper limit of summation over  $j$  instead of  $\infty$ .

## 4. SOLUTION METHODS FOR TD-MFIE

### 4.1. TD-MFIE (1): $h$ and $e$ Formulation

For the TD-MFIE formulation, the electric current  $\mathbf{J}$  and the magnetic current  $\mathbf{M}$  on the dielectric structure may be approximated in terms of two separate spatial basis functions as

$$\mathbf{J}(\mathbf{r}, t) = \sum_{n=1}^N J_n(t) \mathbf{g}_n(\mathbf{r}) \quad (59)$$

$$\mathbf{M}(\mathbf{r}, t) = \sum_{n=1}^N M_n(t) \mathbf{f}_n(\mathbf{r}) \quad (60)$$

where  $J_n$  and  $M_n$  are unknown constants yet to be determined [25]. These expansions are dual to those used in the TD-EFIE formulation of the previous section. By using (9) and (10), we may expand the two electric and magnetic current source vectors as

$$\mathbf{e}(\mathbf{r}, t) = \sum_{n=1}^N e_n(t) \mathbf{g}_n(\mathbf{r}) \quad (61)$$

$$\mathbf{h}(\mathbf{r}, t) = \sum_{n=1}^N h_n(t) \mathbf{f}_n(\mathbf{r}) \quad (62)$$

where  $e_n$  and  $h_n$  are the time domain unknown coefficients to be determined as in the TD-EFIE formulation.

By substituting (61) and (62) into (2) and using the standard definition of the inner product with  $\mathbf{f}_m$  as a testing function, we have

$$\begin{aligned} & \sum_{n=1}^N \sum_{p,q} \left[ \varepsilon_v a_{mn}^{pq} \frac{d^2}{dt^2} h_n(\tau_{mn,v}^{pq}) + \frac{b_{mn}^{pq}}{\mu_v} h_n(\tau_{mn,v}^{pq}) \right] \\ & - \sum_{n=1}^N \left[ c_{mn}^{(v)} \frac{d}{dt} e_n(t) + \sum_{p,q} \left\{ \frac{d_{mn,1}^{pq}}{c_v} \frac{d^2}{dt^2} e_n(\tau_{mn,v}^{pq}) + d_{mn,2}^{pq} \frac{d}{dt} e_n(\tau_{mn,v}^{pq}) \right\} \right] \\ & = V_m^{H(v)}(t) \quad (63) \end{aligned}$$

where the elements in the left-hand side are same as (22)–(25), and

$$V_m^{H(v)}(t) = \begin{cases} V_m^H(t), & v = 1 \\ 0, & v = 2 \end{cases} \quad (64)$$

$$V_m^H(t) = \int_S \mathbf{f}_m(\mathbf{r}) \cdot \mathbf{H}^i(\mathbf{r}, t) dS. \quad (65)$$

The coefficients for the temporal expansion functions  $e_n(t)$  and  $h_n(t)$  introduced in (61) and (62) can be expanded as in (30) and (31).

Substituting the expressions for the basis functions representing the unknown, (30) and (31), and their derivatives into (63), and performing a temporal testing, we get a matrix equation as

$$\begin{bmatrix} \left[ \alpha_{mn}^{H(1)} \right] & \left[ \beta_{mn}^{H(1)} \right] \\ \left[ \alpha_{mn}^{H(2)} \right] & \left[ \beta_{mn}^{H(2)} \right] \end{bmatrix} \begin{bmatrix} [h_{n,i}] \\ [e_{n,i}] \end{bmatrix} = \begin{bmatrix} \left[ \gamma_{m,i}^{H(1)} \right] \\ \left[ \gamma_{m,i}^{H(2)} \right] \end{bmatrix} \quad (66)$$

where

$$\alpha_{mn}^{H(v)} = \sum_{p,q} \left( \frac{s^2 \varepsilon_v a_{mn}^{pq}}{4} + \frac{b_{mn}^{pq}}{\mu_v} \right) \exp \left( -\frac{s R_{mn}^{pq}}{2c_v} \right) \quad (67)$$

$$\beta_{mn}^{H(v)} = - \left[ \frac{s c_{mn}^{(v)}}{2} + \sum_{p,q} \left( \frac{s^2 d_{mn,1}^{pq}}{4 c_v} + \frac{s}{2} d_{mn,2}^{pq} \right) \exp \left( - \frac{s R_{mn}^{pq}}{2 c_v} \right) \right] \quad (68)$$

$$\gamma_{m,i}^{H(v)} = V_{m,i}^{H(v)} + P_{m,i}^{H(v)} + Q_{m,i}^{H(v)} \quad (69)$$

$$V_{m,i}^{H(v)} = \int_0^\infty \phi_i(st) V_m^{H(v)}(t) d(st) \quad (70)$$

$$P_{m,i}^{H(v)} = - \sum_{n=1}^N \sum_{p,q} \left[ \left( \frac{s^2 \varepsilon_v a_{mn}^{pq}}{4} + \frac{b_{mn}^{pq}}{\mu_v} \right) \sum_{j=0}^{i-1} h_{n,j} I_{ij} \left( \frac{s R_{mn}^{pq}}{c_v} \right) + s^2 \varepsilon_v a_{mn}^{pq} \sum_{j=0}^i \sum_{k=0}^{j-1} (j-k) h_{n,k} I_{ij} \left( \frac{s R_{mn}^{pq}}{c_v} \right) \right] \quad (71)$$

$$Q_{m,i}^{H(v)} = \sum_{n=1}^N \left[ s c_{mn}^{(v)} \sum_{k=0}^{i-1} e_{n,k} + \sum_{p,q} \left\{ \left( \frac{s^2 d_{mn,1}^{pq}}{4 c_v} + \frac{s d_{mn,2}^{pq}}{2} \right) \sum_{j=0}^{i-1} e_{n,j} I_{ij} \left( \frac{s R_{mn}^{pq}}{c_v} \right) + \frac{s^2 d_{mn,1}^{pq}}{c_v} \sum_{j=0}^i \sum_{k=0}^{j-1} (j-k) e_{n,k} I_{ij} \left( \frac{s R_{mn}^{pq}}{c_v} \right) + s d_{mn,2}^{pq} \sum_{j=0}^i \sum_{k=0}^{j-1} e_{n,k} I_{ij} \left( \frac{s R_{mn}^{pq}}{c_v} \right) \right\} \right]. \quad (72)$$

By solving the matrix equation (66) in a marching-on in degree procedure with  $M$  temporal basis functions, the electric and magnetic transient current coefficients in (59) and (60) are expressed using the relation (19) and (20) with (30) and (31), respectively. The far scattered electric field at a point  $\mathbf{r}$  is given by

$$\mathbf{E}^s(\mathbf{r}, t) \approx - \frac{1}{8\pi c_1 r} \sum_{n=1}^N l_n \sum_q \left[ \eta_1(\mathbf{n} \times \boldsymbol{\rho}_n^q) \frac{d^2}{dt^2} e_n(\tau_n^q) + \boldsymbol{\rho}_n^q \frac{d^2}{dt^2} h_n(\tau_n^q) \times \hat{\mathbf{r}} \right]. \quad (73)$$

#### 4.2. TD-MFIE (2): $\mathbf{h}$ and $\mathbf{J}$ Formulation

In this section, we present the second method to solve the TD-MFIE using the expansion for the electric current (59) directly instead of

using (61). By following a similar analysis as that for (66), we have a matrix equation

$$\begin{bmatrix} \begin{bmatrix} H^{(1)} \\ \alpha_{mn} \end{bmatrix} & \begin{bmatrix} \beta_{mn}^{H(1)} \end{bmatrix} \\ \begin{bmatrix} H^{(2)} \\ \alpha_{mn} \end{bmatrix} & \begin{bmatrix} \beta_{mn}^{H(2)} \end{bmatrix} \end{bmatrix} \begin{bmatrix} [h_{n,i}] \\ [J_{n,i}] \end{bmatrix} = \begin{bmatrix} \begin{bmatrix} H^{(1)} \\ \gamma_{m,i} \end{bmatrix} \\ \begin{bmatrix} H^{(2)} \\ \gamma_{m,i} \end{bmatrix} \end{bmatrix} \quad (74)$$

where the elements related to the electric current are

$$\beta_{mn}^{H(v)} = - \left[ c_{mn}^{(v)} + \sum_{p,q} \left( \frac{sd_{mn,1}^{pq}}{2c_v} + d_{mn,2}^{pq} \right) \exp \left( -\frac{sR_{mn}^{pq}}{2c_v} \right) \right] \quad (75)$$

$$\begin{aligned} Q_{m,i}^{H(v)} = & \sum_{n=1}^N \sum_{p,q} \left\{ \left( \frac{sd_{mn,1}^{pq}}{2c_v} + d_{mn,2}^{pq} \right) \sum_{j=0}^{i-1} J_{n,j} I_{ij} \left( \frac{sR_{mn}^{pq}}{c_v} \right) \right. \\ & \left. + \frac{sd_{mn,1}^{pq}}{c_v} \sum_{j=0}^i \sum_{k=0}^{j-1} J_{n,k} I_{ij} \left( \frac{sR_{mn}^{pq}}{c_v} \right) \right\} \quad (76) \end{aligned}$$

and other elements are same to those used in (66) in the Section 4.1. Solving (74) by a marching-on in degree procedure with  $M$  temporal basis functions, we can obtain the electric current coefficient directly using the expression as (55). The far field is similar to that in (73), but is modified to yield:

$$\mathbf{E}^s(\mathbf{r}, t) \approx -\frac{1}{8\pi c_1 r} \sum_{n=1}^N l_n \sum_q \left[ \eta_1(\mathbf{n} \times \boldsymbol{\rho}_n^q) \frac{d}{dt} J_n(\tau_n^q) + \boldsymbol{\rho}_n^q \frac{d^2}{dt^2} h_n(\tau_n^q) \times \hat{\mathbf{r}} \right]. \quad (77)$$

### 4.3. TD-MFIE (3): $M$ and $J$ Formulation

In this section, we present the third method using the expansion for the equivalent currents directly instead of using the two source vectors. Taking a derivative with respect to time, we derive the following integral equations from (2)

$$\begin{aligned} & \left[ \frac{\partial^2}{\partial t^2} \mathbf{F}_v(\mathbf{r}, t) + \nabla \frac{\partial}{\partial t} \Phi_v(\mathbf{r}, t) - \frac{1}{\mu_v} \nabla \times \frac{\partial}{\partial t} \mathbf{A}_v(\mathbf{r}, t) \right]_{\tan} \\ & = \begin{cases} \left[ \frac{\partial}{\partial t} \mathbf{H}^i(\mathbf{r}, t) \right]_{\tan} & v = 1 \\ 0, & v = 2 \end{cases} \quad \mathbf{r} \in S. \quad (78) \end{aligned}$$

Using (59) and (60), the time domain electric and magnetic current coefficients are expanded as in (49) and (55). Substituting (49) and

(55) with (59) and (60) into (78), and following a similar procedure as that for (66), we have a matrix equation

$$\begin{bmatrix} \begin{bmatrix} \alpha_{mn}^{H(1)} \\ \alpha_{mn}^{H(1)} \end{bmatrix} & \begin{bmatrix} \beta_{mn}^{H(1)} \\ \beta_{mn}^{H(1)} \end{bmatrix} \end{bmatrix} \begin{bmatrix} [M_{n,i}] \\ [J_{n,i}] \end{bmatrix} = \begin{bmatrix} \begin{bmatrix} \gamma_{m,i}^{H(1)} \\ \gamma_{m,i}^{H(2)} \end{bmatrix} \end{bmatrix} \quad (79)$$

where the impedance matrix elements in the left hand side are same as those used in (66) of the previous Section 4.1. The elements related to the right hand side are obtained by replacing  $J_{n,j}$  and  $M_{n,j}$  instead of  $e_{n,j}$  and  $h_{n,j}$  in (69)–(72), respectively, and

$$V_m^H(t) = \int_S \mathbf{f}_m(\mathbf{r}) \cdot \frac{\partial}{\partial t} \mathbf{H}^i(\mathbf{r}, t) dS. \quad (80)$$

By solving (79) with a marching-on in degree algorithm with  $M$  temporal basis functions, we can obtain the electric and magnetic current coefficients directly as given in (55) and (49) by replacing the summation over  $\infty$  with  $M - 1$ . The far field is obtained through a similar expression as in (73), where

$$\mathbf{E}^s(\mathbf{r}, t) \approx -\frac{1}{8\pi c_1 r} \sum_{n=1}^N l_n \sum_q \left[ \eta_1 (\mathbf{n} \times \boldsymbol{\rho}_n^q) \frac{d}{dt} J_n(\tau_n^q) + \boldsymbol{\rho}_n^q \frac{d}{dt} M_n(\tau_n^q) \times \hat{\mathbf{r}} \right]. \quad (81)$$

## 5. NUMERICAL EXAMPLE

We present the numerical results for 3-D dielectric scatterers with a relative permittivity  $\epsilon_r = 2$ , placed in free space. In this section,  $c$  and  $\eta$  mean the speed of the wave propagation and the wave impedance of the free space, respectively. The scatterers are illuminated by a Gaussian plane wave, in which the electromagnetic fields are given by

$$\mathbf{E}^i(\mathbf{r}, t) = \mathbf{E}_0 \frac{4}{\sqrt{\pi T}} e^{-\gamma^2}, \quad \mathbf{H}^i(\mathbf{r}, t) = \frac{1}{\eta} \hat{\mathbf{k}} \times \mathbf{E}^i(\mathbf{r}, t) \quad (82)$$

where  $\gamma = (4/T)(ct - ct_0 - \mathbf{r} \cdot \hat{\mathbf{k}})$ ,  $\hat{\mathbf{k}}$  is the unit vector in the direction of the wave propagation,  $T$  is the width of the Gaussian pulse in *light meter* (lm), and  $t_0$  is a time delay which represents the time at which the pulse peaks at the origin. One *light meter* is the length of time taken by the electromagnetic wave to travel 1 m in the free space. In this work, the field is incident from  $\phi = 0^\circ$  and  $\theta = 0^\circ$  with  $\hat{\mathbf{k}} = -\hat{\mathbf{z}}$ , and  $\mathbf{E}_0 = \hat{\mathbf{x}}$ . In the numerical computation, we use a Gaussian pulse

of  $T = 4$  nm and  $ct_0 = 6$  nm. We set  $s = 10^9$  and  $M = 80$ . When we consider a signal with time duration  $T_f$  in the time domain, we note that the upper limit of the integral in (31) and (39) can be replaced by the time duration  $sT_f$  instead of infinity. Here we set  $sT_f = 40$  nm. All the solutions computed by our presented method are compared with the inverse discrete Fourier transform (IDFT) of the solutions by the frequency domain electric field integral equation (FD-EFIE) and frequency domain magnetic field integral equation (FD-MFIE) formulations described in [25] in the range of 0–500 MHz intervals with 128 samples. The shaded patches included in the figures indicate the location of the current to be observed associated with the common edge. The far field solutions are  $\theta$ - (or  $x$ -) components of electric field taken along the backward direction ( $+z$  axis) from the scatterers.

As a first example, we consider a dielectric sphere of radius 0.5 m centered at the origin. This has a total of 528 patches and 792 edges as shown in Fig. 2. Fig. 2(a) and 2(b) show the transient responses for the  $\theta$ -directed electric and magnetic current densities on the sphere at  $(\theta = 90^\circ, \phi = 7.5^\circ)$  and  $(\theta = 82.5^\circ, \phi = 90^\circ)$ , respectively, computed by the present TD-EFIE formulations and compared with the IDFT of the FD-EFIE solutions. We can see that the three solutions of electric and magnetic currents by the present TD-EFIE methods are stable and are in agreement with the IDFT solutions. Fig. 3 shows the transient response for the  $\theta$ -directed electric and magnetic current densities on the sphere at  $(\theta = 82.5^\circ, \phi = 0^\circ)$  and  $(\theta = 90^\circ, \phi = 97.5^\circ)$ , respectively. They are computed by the present TD-MFIE formulations and compared with the IDFT of the FD-MFIE solutions. We can see that the three solutions for the electric and magnetic currents by the present TD-MFIE methods are stable and the agreement with the IDFT of the FD-MFIE solutions is good. Because of using the different spatial basis functions to expand the equivalent currents in EFIE and MFIE, we do not compare Figs. 2 and 3 directly. However, the locations to be observed are near, so we can see that the shapes of the current responses in Figs. 2(a) and 2(b) are similar to Figs. 3(a) and 3(b), respectively.

Now, we show several examples of far field response from the various dielectric structures from Fig. 4 to Fig. 8. Fig. 4 presents the transient response for the backward scattered far field from the dielectric sphere by using the TD-EFIE and TD-MFIE techniques just presented, along with the Mie series and the IDFT solutions. All the solutions agree well as is evident from Figs. 4(a) and 4(b), respectively. We note that EFIE and MFIE provide the same solutions by comparing them with the Mie solution in each figure. Next, we consider a dielectric cube, 1 m on a side, centered at the origin as shown in Fig. 5.

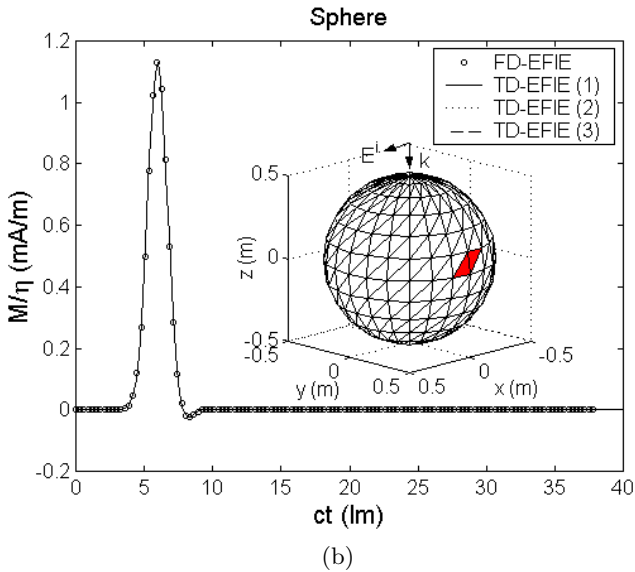
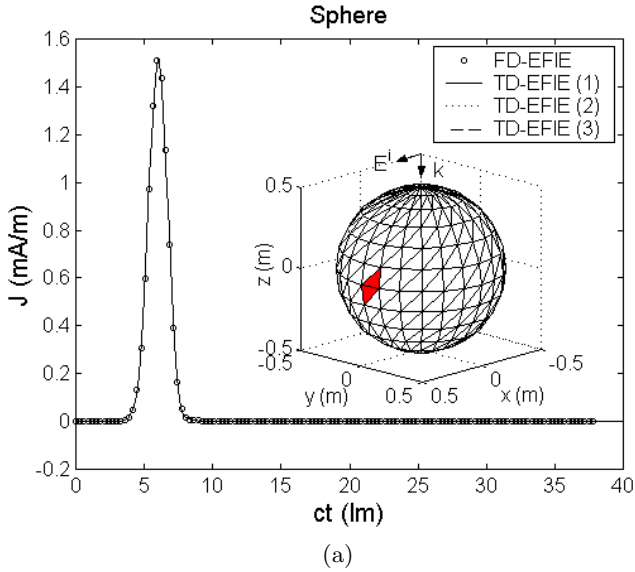


**Figure 2.** Transient current on the dielectric sphere computed by the electric field integral equation. (a)  $\theta$ -directed electric current. (b)  $\theta$ -directed magnetic current.

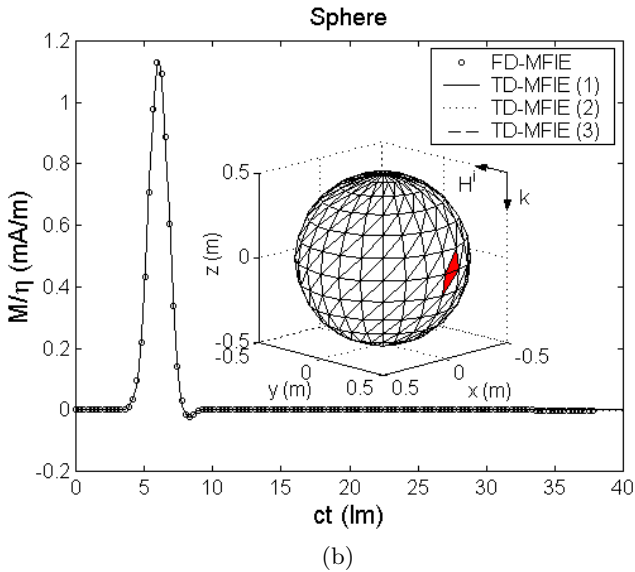
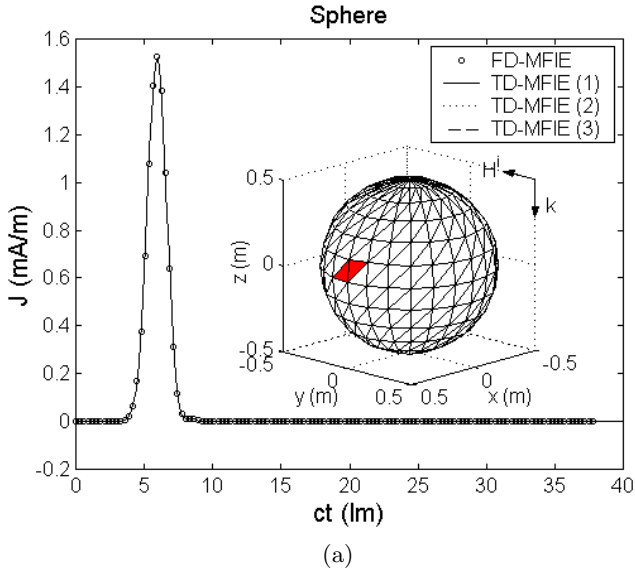


**Figure 3.** Transient current on the dielectric sphere computed by the magnetic field integral equation. (a)  $\theta$ -directed electric current. (b)  $\theta$ -directed magnetic current.

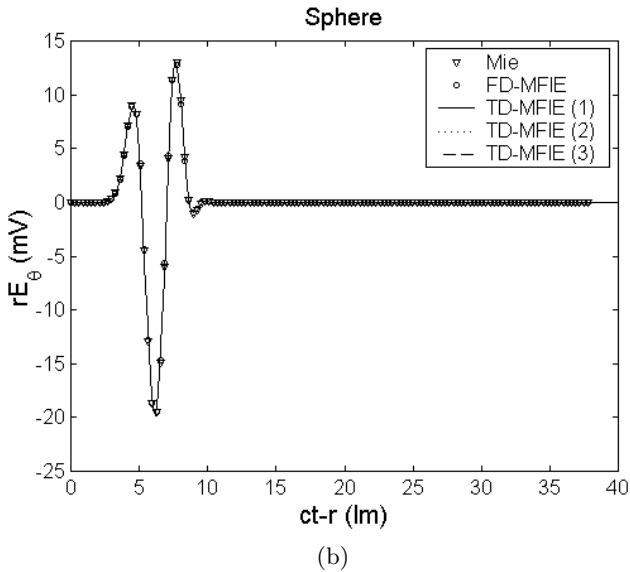
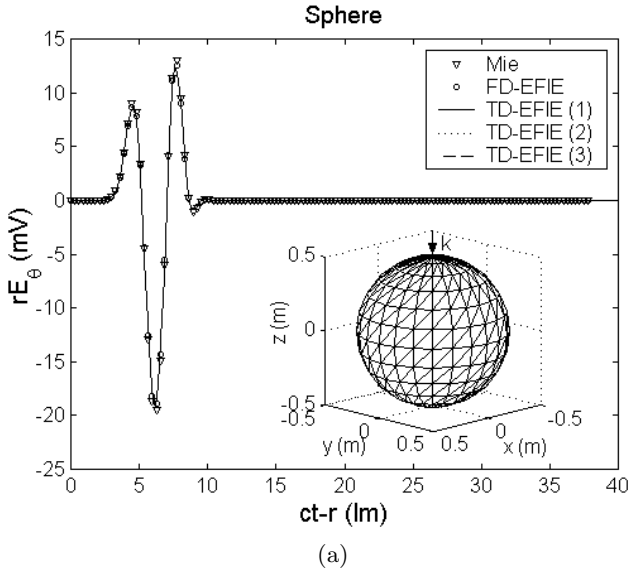


**Figure 4.** Scattered far field from the dielectric sphere along the backward direction. (a) Electric field integral equation. (b) Magnetic field integral equation.

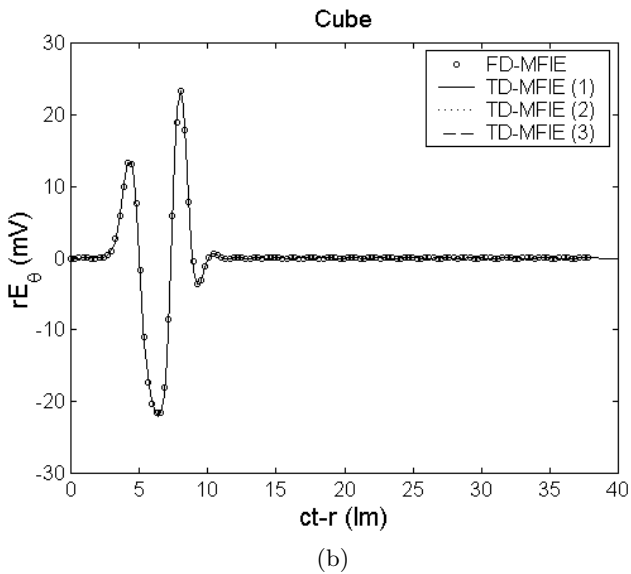
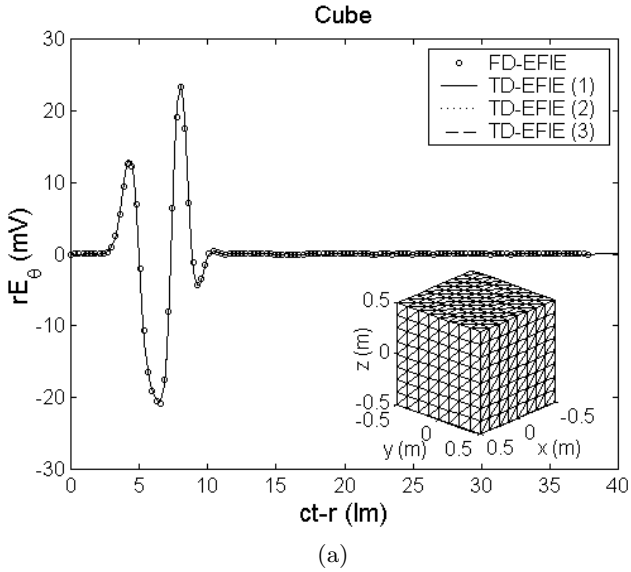


**Figure 5.** Scattered far field from the dielectric cube along the backward direction. (a) Electric field integral equation. (b) Magnetic field integral equation.

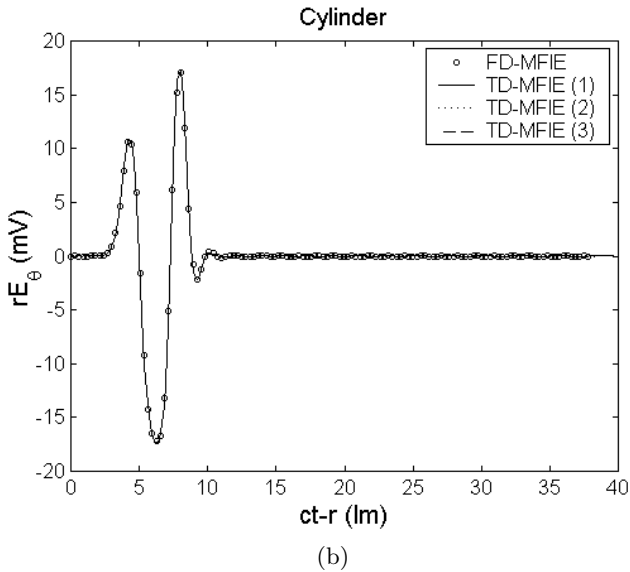
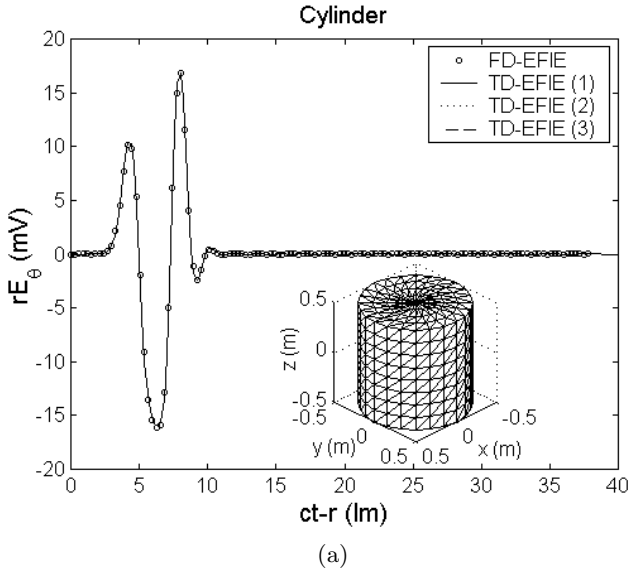


**Figure 6.** Scattered far field from the dielectric cylinder along the backward direction. (a) Electric field integral equation. (b) Magnetic field integral equation.

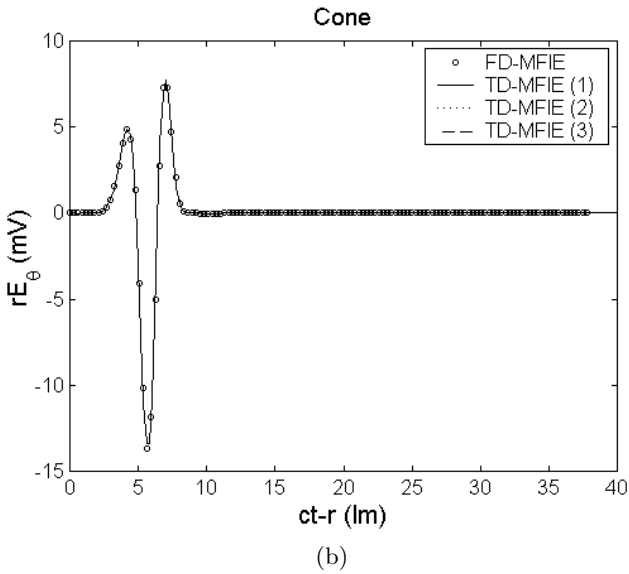
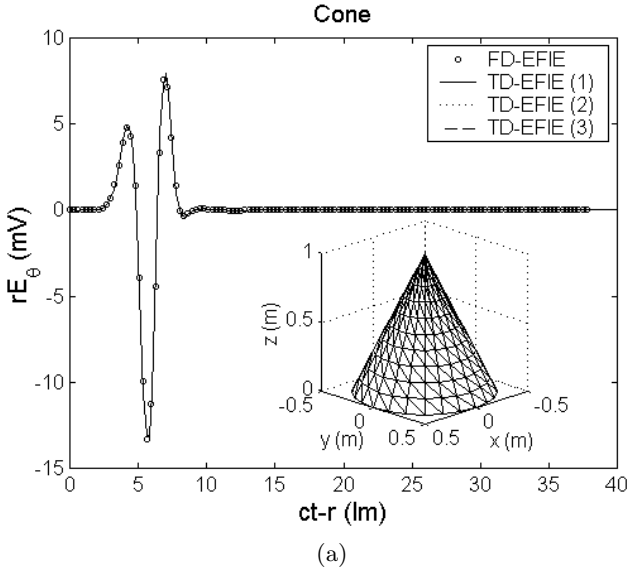


**Figure 7.** Scattered far field from the dielectric cone along the backward direction. (a) Electric field integral equation. (b) Magnetic field integral equation.

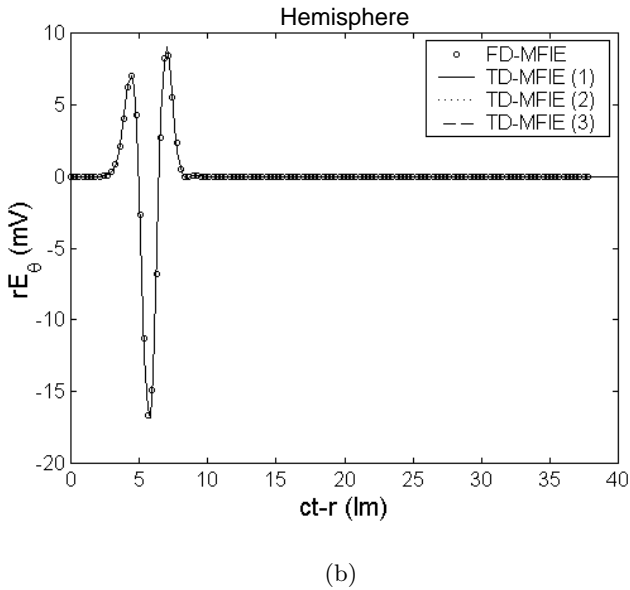
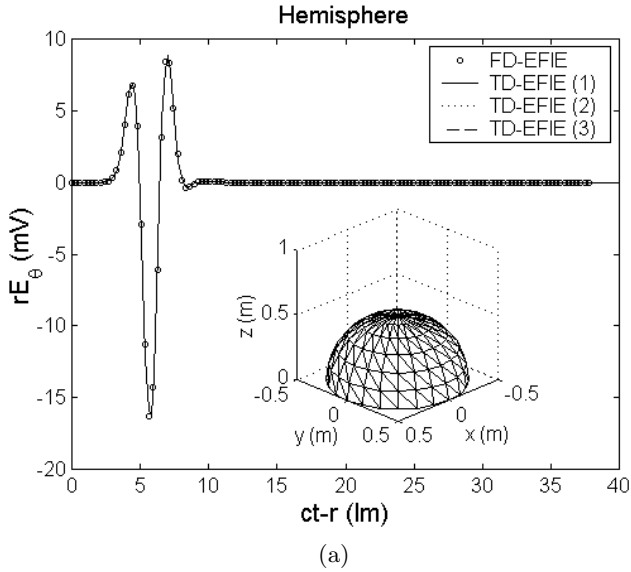


**Figure 8.** Scattered far field from the dielectric hemisphere along the backward direction. (a) Electric field integral equation. (b) Magnetic field integral equation.

This has a total of 768 patches and 1,152 edges. Fig. 5 presents the transient response for the far field from the dielectric cube with the IDFT solution. The transient responses for the far field computed by the proposed methods are stable. All the three solutions of TD-EFIE and TD-MFIE agree well as is evident from the Figs. 5(a) and 5(b), respectively. The next structure to be analyzed is the dielectric cylinder centered at the origin, which is shown in Fig. 6. The radius of the cylinder is 0.5 m and the height along the  $z$ -direction is 1 m. This structure is divided into 720 triangular patches with a total number of 1,080 edges. In Fig. 6, the back-scattered fields computed by our proposed methods are compared with the IDFT results. Fig. 7 shows the far field from a dielectric cone, which has a base of 0.5 m radius placed at  $z = 0$  and 1 m height along the  $z$ -direction. This cone is divided into 624 triangular patches with a total number of 936 edges. Back-scattered far-zone fields obtained using the proposed methods are stable. A good agreement between the four results is evident for this example. Fig. 8 presents the transient response for the far field from a dielectric hemisphere with the IDFT solutions using FD-EFIE and FD-MFIE. The hemisphere has a radius of 0.5 m. This has a total of 432 patches and 648 edges. The transient responses for the far field computed by the proposed methods are stable. All the three solutions agree well as is evident from the figure and it is difficult to distinguish between the presented results.

## 6. CONCLUSION

We have investigated various methods to solve the time-domain electric and magnetic field integral equations for scattering from three-dimensional arbitrarily shaped dielectric structures. To apply a MoM procedure, we used the triangular patch vector function and its orthogonal component as spatial basis functions. Because of the use of different spatial basis functions, the electric and magnetic field integral equations cannot be combined into a combined field integral equation. We introduced a temporal basis function set derived from the Laguerre polynomials. The advantage of the proposed method is to guarantee late-time stability. With the representation of the derivative of the transient coefficient in an analytic form, the temporal derivative in the integral equation can be treated analytically. In addition, the time variable can be integrated out completely and one now solves the problem only in space. Transient equivalent currents and far fields obtained by the present methods in this paper are accurate and stable. The agreement of all the transient solutions and the frequency domain solutions is excellent. The formulations to be considered in this paper

are useful for analyzing the transient scattering from dielectric objects when the spectrum of the incident signal does not contain any internal resonant frequency of the structure.

## ACKNOWLEDGMENT

This work was supported by grant No. R05-2004-000-10063-0 from Ministry of Science & Technology, Korea.

## REFERENCES

1. Rao, S. M., *Time Domain Electromagnetics*, Academic Press, 1999.
2. Mieras, H. and C. L. Bennet, "Space-time integral equation approach to dielectric targets," *IEEE Trans. Antennas Propagat.*, Vol. 30, 2–9, Jan. 1982.
3. Vechinski, D. A., S. M. Rao, and T. K. Sarkar, "Transient scattering from three-dimensional arbitrary shaped dielectric bodies," *J. Opt. Soc. Amer.*, Vol. 11, No. 4, 1458–1470, April 1994.
4. Rynne, B. P., "Time domain scattering from dielectric bodies," *Electromagn.*, Vol. 14, 181–193, 1994.
5. Marx, E., "Integral equation for scattering by a dielectric," *IEEE Trans. Antennas Propagat.*, Vol. 32, 166–172, Feb. 1984.
6. Pocock, M. D., M. J. Bluck, and S. P. Walker, "Electromagnetic scattering from 3-D curved dielectric bodies using time domain integral equations," *IEEE Trans. Antennas Propagat.*, Vol. 46, No. 8, 1212–1219, Aug. 1998.
7. Sarkar, T. K., W. Lee, and S. M. Rao, "Analysis of transient scattering from composite arbitrarily shaped complex structures," *IEEE Trans. Antennas Propagat.*, Vol. 48, No. 10, 1625–1634, Oct. 2000.
8. Jung, B. H. and T. K. Sarkar, "Time-domain electric-field integral equation with central finite difference," *Microwave Opt. Technol. Lett.*, Vol. 31, No. 6, 429–435, Dec. 2001.
9. Gres, N. T., A. A. Ergin, E. Michielssen, and B. Shanker, "Volume-integral-equation based analysis of transient electromagnetic scattering from three-dimensional inhomogeneous dielectric objects," *Radio Sci.*, Vol. 36, No. 3, 379–386, May–June 2001.
10. Rao, S. M. and T. K. Sarkar, "Implicit solution of time-

- domain integral equations for arbitrarily shaped dielectric bodies,” *Microwave Opt. Technol. Lett.*, Vol. 21, No. 3, 201–205, May 1999.
11. Chung, Y.-S., T. K. Sarkar, and B. H. Jung, “Solution of time domain electric field integral equation for arbitrarily shaped dielectric bodies using an unconditionally stable methodology,” *Radio Sci.*, Vol. 38, No. 3, 14.1–12, May–June 2003.
  12. Sarkar, T. K. and J. Koh, “Generation of a wide-band electromagnetic response through a Laguerre expansion using early-time and low-frequency data,” *IEEE Trans. Microwave Theory Tech.*, Vol. 50, No. 5 1408–1416, May 2002.
  13. Rao, S. M., D. R. Wilton, and A. W. Glisson, “Electromagnetic scattering by surfaces of arbitrary shape,” *IEEE Trans. Antennas Propagat.*, Vol. 30, No. 3, 409–418, May 1982.
  14. Sarkar, T. K., S. M. Rao, and A. R. Djordjevic, “Electromagnetic scattering and radiation from finite microstrip structures,” *IEEE Trans. Microwave Theory Tech.*, Vol. 38, No. 11, 1568–1575, Nov. 1990.
  15. Rao, S. M. and D. R. Wilton, “E-field, H-field, and combined field solution for arbitrarily shaped three-dimensional dielectric bodies,” *Electromagn.*, Vol. 10, 407–421, 1990.
  16. Jung, B. H., Y.-S. Chung, and T. K. Sarkar, “Time-domain EFIE, MFIE, and CFIE formulations using Laguerre polynomials as temporal basis functions for the analysis of transient scattering from arbitrary shaped conducting structures,” *J. of Electromagn. Waves and Applicat.*, Vol. 17, No. 5, 737–739, 2003.
  17. Rao, S. M., “Electromagnetic scattering and radiation of arbitrarily-shaped surfaces by triangular patch modeling,” Ph.D. Dissertation, Univ. Mississippi, Aug. 1980.
  18. Wilton, D. R., S. M. Rao, A. W. Glisson, D. H. Schaubert, O. M. Al-Bundak, and C. M. Butler, “Potential integrals for uniform and linear source distributions on polygonal and polyhedral domains,” *IEEE Trans. Antennas Propagat.*, Vol. 32, No. 3, 276–281, March 1984.
  19. Graglia, R. D., “Static and dynamic potential integrals for linearly varying source distributions in two- and three-dimensional problems,” *IEEE Trans. Antennas Propagat.*, Vol. 35, No. 6, 662–669, June 1987.
  20. Caorsi, S., D. Moreno, and F. Sidoti, “Theoretical and numerical treatment of surface integrals involving the free-space Green’s function,” *IEEE Trans. Antennas Propagat.*, Vol. 41, No. 9, 1296–1301, Sept. 1993.

21. Graglia, R. D., "On the numerical integration of the linear shape functions times the 3-D Green's function or its gradient on a plane triangle," *IEEE Trans. Antennas Propagat.*, Vol. 41, No. 10, 1448–1455, Oct. 1993.
22. Eibert, T. F. and V. Hansen, "On the calculation of potential integrals for linear source distributions on triangular domains," *IEEE Trans. Antennas Propagat.*, Vol. 43, No. 12, 1499–1502, Dec. 1995.
23. Hodges, R. E. and Y. Rahmat-Samii, "The evaluation of MFIE integrals with the use of vector triangle basis functions," *Microwave Opt. Technol. Lett.*, Vol. 14, No. 1, 9–14, Jan. 1997.
24. Poularikas, A. D., *The Transforms and Applications Handbook* IEEE Press, 1996.
25. Jung, B. H., T. K. Sarkar, and Y.-S. Chung, "A survey of various frequency domain integral equations for the analysis of scattering from three-dimensional dielectric objects," *J. of Electromagn. Waves and Applicat.*, Vol. 16, No. 10, 1419–1421, 2002.

**Baek Ho Jung** received the B.S., M.S., and Ph.D. degrees in Electronic and Electrical Engineering from Kyungpook National University, Taegu, Korea, in 1986, 1989, and 1997, respectively. From 1989 to 1994, he was a researcher at Agency for Defense Development in Korea. Since 1997, he has been a Lecturer and currently an Assistant Professor in the Department of Information and Communication Engineering, Hoseo University, Asan, Korea. He is now in Syracuse University, NY as a visiting scholar from 2001 to 2003. His current interests are in computational electromagnetics and wave propagation.

**Tapan Kumar Sarkar** received the B.Tech. degree from the Indian Institute of Technology, Kharagpur, India, in 1969, the M.Sc.E. degree from the University of New Brunswick, Fredericton, Canada, in 1971, and the M.S. and Ph.D. degrees from Syracuse University; Syracuse, New York in 1975. From 1975 to 1976 he was with the TACO Division of the General Instruments Corporation. He was with the Rochester Institute of Technology, Rochester, NY, from 1976 to 1985. He was a Research Fellow at the Gordon McKay Laboratory, Harvard University, Cambridge, MA, from 1977 to 1978. He is now a Professor in the Department of Electrical and Computer Engineering, Syracuse University; Syracuse, NY. His current research interests deal with numerical solutions of operator equations arising in electromagnetics and signal processing with application to system design. He obtained one of the "best solution" awards in May 1977 at the Rome Air Development Center (RADC) Spectral Estimation Workshop. He has

authored or coauthored more than 210 journal articles and numerous conference papers and has written chapters 28 books and ten books including the latest one *Iterative and Self Adaptive Finite-Elements in Electromagnetic Modeling* which was published in 1998 by Artech House. Dr. Sarkar is a registered professional engineer in the State of New York. He received the Best Paper Award of the IEEE Transactions on Electromagnetic Compatibility in 1979 and in the 1997 National Radar Conference. He received the College of Engineering Research Award in 1996 and the chancellor's citation for excellence in research in 1998 at Syracuse University. He was an Associate Editor for feature articles of the IEEE Antennas and Propagation Society Newsletter, and he was the Technical Program Chairman for the 1988 IEEE Antennas and Propagation Society International Symposium and URSI Radio Science Meeting. He is on the editorial board of Journal of Electromagnetic Waves and Applications and Microwave and Optical Technology Letters. He has been appointed U.S. Research Council Representative to many URSI General Assemblies. He was the Chairman of the Intercommission Working Group of International URSI on Time Domain Metrology (1990–1996). Dr. Sarkar is a member of Sigma Xi and International Union of Radio Science Commissions A and B. He received the title Docteur Honoris Causa from Universite Blaise Pascal, Clermont Ferrand, France in 1998 and the medal of the City Clermont Ferrand, France in 2000.

**Magdalena Salazar-Palma** was born in Granada, Spain. She received the degree and Ph.D. degree in Ingeniero de Telecomunicación from the Universidad Politécnica de Madrid (Spain). She is a Professor Titular of the Departamento de Señales, Sistemas y Radiocomunicaciones (Signals, Systems and Radiocommunications Department) (SSR) at the Escuela Técnica Superior de Ingenieros de Telecomunicación (School for Telecommunication Engineering) of the same university. She has developed her research within the Grupo de Microondas y Radar (Microwave and Radar Group) of the SSR Department in the areas of electromagnetic field theory; computational and numerical methods for microwave passive components, and antenna analysis; design, simulation, optimization, implementation, and measurements of microwave circuits both in waveguide and integrated (hybrid and monolithic) technologies; and network and filter theory and design. She has authored 3 books published by international editorial companies, 15 contributions for chapters and articles in books published by international editorial companies, 30 papers in international scientific journals, 140 papers in international conferences, symposiums, and workshops. She is associated editor

for the IEEE Antennas and Wireless Propagation Letters. She has received two individual research awards and, together with the rest of her Department, another research award, all from national institutions. From 1992 up to 1996 she served as Chairperson of the IEEE Spain Section AP-S/MTT-S Joint Chapter. From January 1997 up to December 2001 she was Chairperson of IEEE Spain Section. In January 2003 she was appointed as Chairperson of IEEE WIEC where she is currently serving.